ASTRONOMY & ASTROPHYSICS
SUPPLEMENT SERIES

NOVEMBER I **2000**, PAGE 481

Astron. Astrophys. Suppl. Ser. **146**, 481–498 (2000)

He($1\,^1$S, $2\,^3$S, $2\,^1$S, $2\,^3$P $\rightarrow$ $n\,^{1,3}L$): Thermally averaged electron collision strengths for $n \leq 5$

I. Bray[1], **A. Burgess**[2], **D.V. Fursa**[1], **and J.A. Tully**[3]

[1] Department of Physics, The Flinders University of South Australia, P.O. Box 2100, Adelaide 5001, Australia
[2] Department of Applied Mathematics and Theoretical Physics, Silver Street, Cambridge CB3 9EW, UK
[3] Département Gian Domenico Cassini, Observatoire de la Côte d'Azur, BP 4229, 06304 Nice Cedex 4, France

Received March 2; accepted August 16, 2000

Abstract. We present thermally averaged collision strengths for electron induced transitions in helium from $1s^2\ ^1$S, 1s2s ^{1,3}S, 1s2p ^{3}P to higher lying terms $1snl\ ^{1,3}L$ with $n \leq 5$. Results are tabulated as functions of temperature in the range $3.75 \leq \log T \leq 5.75$. Cross sections are calculated using the convergent close-coupling (CCC) method.

Key words: atomic data

1. Introduction

Helium has been of interest to astronomers for over 130 years ever since it was discovered spectroscopically in the Sun's atmosphere. The bright yellow D^3 chromospheric line, which Lockyer (1869a,b,c) saw in full sunlight near the limb on the 20th of October 1868, was later identified with the $4\,^3$D $\rightarrow$ $3\,^3$P transition (587.6 nm) in He I.

Bartschat (1998) gives a concise summary of the recent evolution of our understanding of electron excitation of helium, the process to which the present paper is devoted; the list of references he provides is particularly useful.

Quantum mechanics provides the means of investigating how atomic helium behaves when bombarded by electrons, and there has been much effort made to quantify this since the advent of electronic computers. The convergent close-coupling (CCC) method for calculating electron-helium collisions has been developed by Fursa & Bray (1995), and has proved to be one of the most successful to date. Astrophysicists are interested in obtaining rate coefficients for collisional excitation and it is with these quantities that the present paper is concerned.

Send offprint requests to: J.A. Tully, e-mail: tully@obs-azur.fr

Bartschat (1998, 1999) has treated some of the transitions dealt with here using the R-matrix with pseudo states (RMPS) approximation (Bartschat et al. 1996). Since his results are for electron energies not exceeding 40 eV with respect to the ground state, they can only provide reliable rate coefficients for temperatures below 20 thousand degrees. Bartschat's cross sections have, however, one advantage over ours in that they are delineated in great detail by the use he made of a very fine energy mesh.

The temperature dependent rate coefficient $q(i \rightarrow j)$ for a transition between atomic terms with indices i and j and energy separation E_{ij} is given by

$$q(i \rightarrow j) = \frac{2\pi^{1/2} a_0 \hbar}{m_\mathrm{e}} \left[\frac{\mathrm{Ry}}{kT}\right]^{1/2} \exp(-E_{ij}/kT) \frac{\Upsilon(i-j)}{\omega_i} \quad (1)$$

where $2\pi^{1/2} a_0\, \hbar\, m_\mathrm{e}^{-1} = 3.610\ 10^{-24}$ m^3 s^{-1}. For energies we use the Rydberg unit, which has the value Ry = 13.6058 eV, while the Boltzmann constant is given by $k = 8.617\ 10^{-5}$ eV deg^{-1}, the temperature T being in degrees Kelvin. The factor $\omega_i = (2S_i + 1)(2L_i + 1)$ is the statistical weight of the i-th term or level. The effective collision strength $\Upsilon(i-j)$ in Eq. (1) was first introduced by Seaton (1953) who defined it as follows:

$$\Upsilon(i-j) = \int_0^\infty \Omega(i-j) \exp(-E_j/kT)\, \mathrm{d}(E_j/kT) \quad (2)$$

where E_j is the energy of the colliding electron after excitation has occurred. The energy dependent collision strength $\Omega(i-j)$ and cross section $Q(i \rightarrow j)$ are related as follows:

$$Q(i \rightarrow j) = \frac{\pi\, \Omega(i-j)}{\omega_i\, k_i^2} \quad (3)$$

where k_i is the wave number of the colliding electron incident on the target atom in level i.

Table 1. Helium term energies in Ry. Observed: Martin (1973); theoretical: FC (frozen core), FCFH (frozen core Hartree Fock)

i	Term	Martin	FC	FCHF
1	$1\,^1$S	0.000000	0.000000	0.000000
2	$2\,^3$S	1.456717	1.396698	1.396522
3	$2\,^1$S	1.515236	1.458400	1.458115
4	$2\,^3$P	1.540783	1.482000	1.482374
5	$2\,^1$P	1.559496	1.499698	1.500117
6	$3\,^3$S	1.669780	1.607601	1.608044
7	$3\,^1$S	1.684619	1.623498	1.623877
8	$3\,^3$P	1.690993	1.629400	1.629850
9	$3\,^3$D	1.695887	1.633501	1.633869
10	$3\,^1$D	1.695916	1.633501	1.633921
11	$3\,^1$P	1.696871	1.635104	1.635658
12	$4\,^3$S	1.734128	1.671698	1.672261
13	$4\,^1$S	1.739978	1.678005	1.678419
14	$4\,^3$P	1.742499	1.680401	1.680772
15	$4\,^3$D	1.744572	1.682098	1.682494
16	$4\,^1$D	1.744594	1.682098	1.682524
17	$4\,^3$F	1.744645	1.682098	1.682514
18	$4\,^1$F	1.744645	1.682098	1.682514
19	$4\,^1$P	1.745013	1.682804	1.683219
20	$5\,^3$S	1.761910	1.699400	1.699848
21	$5\,^1$S	1.764798	1.702604	1.702952
22	$5\,^3$P	1.766048	1.703699	1.704116
23	$5\,^3$D	1.767106	1.704603	1.705002
24	$5\,^1$D	1.767121	1.704603	1.705019
25	$5\,^3$F	1.767143	1.704603	1.705013
26	$5\,^1$F	1.767143	1.704603	1.705013
27	$5\,^3$G	1.767150	1.704603	
28	$5\,^1$G	1.767150	1.704603	
29	$5\,^1$P	1.767334	1.705000	1.705379
30	$6\,^3$S	1.776389	1.714504	1.714299
31	$6\,^1$S	1.778021	1.716701	1.716057
32	$6\,^3$P	1.778734	1.717598	1.716714
33	$6\,^3$D	1.779344	1.717003	1.717228
34	$6\,^1$D	1.779351	1.717003	1.717239
35	$6\,^3$F	1.779366	1.716804	1.717236
36	$6\,^1$F	1.779366	1.716804	1.717236
37	$6\,^3$G	1.779366	1.716804	
38	$6\,^1$G	1.779366	1.716804	
39	$6\,^1$P	1.779483	1.718598	1.717448

2. Energy levels

In Table 1 we list the observed energies of the helium terms which enter into the present calculation of cross sections, our source being Martin's (1973) tabulation. Table 1 also has the frozen-core (FC) theoretical energies used in our collision calculation. For comparison we show the frozen-core Hartree-Fock (FCHF) energies calculated by McEachran (1972); see also Cohen & McEachran (1967a,b) and McEachran & Cohen (1969) where some of these results and discussion of the method can be found.

3. Calculation of cross sections

The details of the CCC approach to e-He scattering have been given by Fursa & Bray (1995). The method is based on the close-coupling (CC) antisymmetric expansion of the total wave function using the He target states. These states are constructed using the frozen-core approximation where all two-electron configurations have one of the electrons described by the He^+ 1s wave function. The other electron function is obtained as a linear combination of an orthogonal Laguerre basis upon diagonalization of the target Hamiltonian. The strength of this approach is that convergence, in say the cross section of interest, may be studied systematically by increasing the Laguerre basis sizes. One disadvantage is that the energy levels for the low-lying states are not as accurate as they could be if the frozen-core approximation was relaxed a little. We have not done so here because such a relaxation results in many more states to be used in the CC formalism requiring some judicious truncating.

In performing the presented calculations a total of 89 states were used that span the discrete spectrum reasonably accurately for states with principal quantum number $n \leq 6$. In addition, the target one-electron continuum was very accurately described. Integrated cross sections were obtained for the $n_i \rightarrow n_f$ transitions with $n_i \leq 5$. The strength of the CCC formalism is to be able to solve large-scale CC equations at any incident energy. However, presently this has to be done from scratch for each energy. Hence, the R-matrix approach is much more efficient in generating cross sections on a fine energy mesh. We have chosen a sufficiently fine mesh so that the relevant integrals, over the energy, could be evaluated to a satisfactory accuracy. The present calculations have been carried out for electron energies that extend as far as 500 eV relative to the ground state. There is no difficulty in extending the calculations as far as say 1 keV.

4. Thermal averaging collision strengths

The CCC program furnishes the cross section $Q(i \rightarrow j)$ as a function of E_i, the collision energy relative to term i. We convert this to a table of $\Omega(i-j)$ as a function of E_j which we then use to calculate $\Upsilon(i-j)$ from Eq. (2) by means of the linear interpolation technique (Burgess & Tully 1992). The upper limit of the integral (2) is replaced by the value of E_j corresponding to the highest value of E_i at which the cross section $Q(i \rightarrow j)$ is calculated by the CCC program. We checked to make sure that the contribution from higher energies was negligible. In order to extend our tabulation of Υ to temperatures well

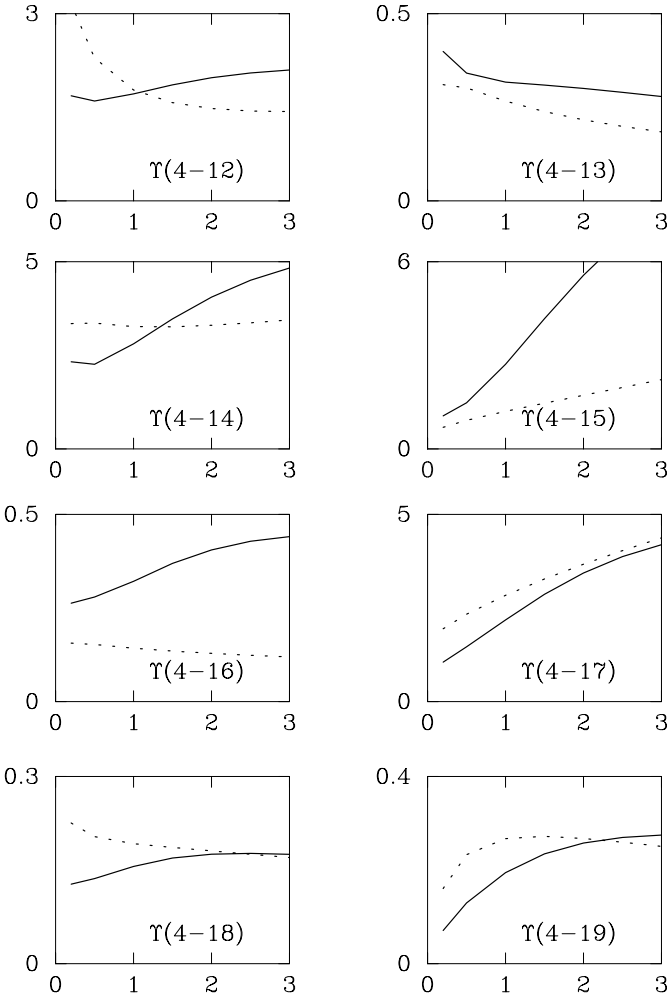

Fig. 1. Effective collision strengths vs. $T/10^4$. Full line, Sawey & Berrington (1993); dashed line, present results

beyond 500 000 degrees it will be necessary to calculate or estimate collision strengths at higher energies than those considered here. Alternatively one could make use of the technique developed by Burgess & Tully (1992) in order to extrapolate the present data up to higher temperatures.

Until now the best source of effective collision strengths has been Sawey & Berrington (1993) – hereafter SB – their data being based on a 29-state R-matrix calculation (Sawey et al. 1990). Using SB's tables one can obtain electron rate coefficients for 157 of the 171 transitions that exist between levels with principal quantum number $n \leq 4$. This tabulation is an improvement on the one produced by Berrington & Kingston (1987) – hereafter BK – from a 19-state R-matrix calculation for transitions between levels with $n \leq 3$. During a workshop for assessing atomic data, which was held in Saint Catherine's College Oxford in 1987, Pradhan (1987) had this to say about the reliability of their data: "For neutral helium the work by Berrington & Kingston, which included the $n = 4$ levels, is rated as having an uncertainty of 10% for excitation to the $n = 2$ states and an uncertainty of 30% for transitions to the $n = 3$ states".

The tabulations of $\Upsilon(T)$ in BK and in SB extend only as far as 30 000 degrees. There are, however, astrophysical situations where helium rate coefficients are needed at temperatures of the order of 120 000 degrees (Bouret 1998); and in the domain of controlled thermonuclear research Summers (1999) tells us that experiments are being performed in which neutral helium is used as a diagnostic tool by being injected into plasmas where the electron temperature can be as high as 10^7 degrees.

The CCC approximation is not subject to the restrictions which limit the R-matrix method with increasing collision energy. As a result we are able to obtain converged cross sections when $E_1 \leq 500$ eV. After being thermally averaged these provide rate coefficients for temperatures up to about 500 000 degrees.

In Tables $2-5$ we give effective collision strengths Υ over the temperature range $3.75 \leq \log T \leq 5.75$. Because of the uncertainty that pseudo resonances introduce into our cross sections at energies close to threshold, we limit the low temperature end of our tabulation to about 6 000 degrees. Some values of Υ in Tables $2-5$ are given in the form a^b, where b denotes the power of 10 by which a should be multiplied. In Fig. 1 we compare our results with those of SB for excitation from $2\,^3\mathrm{P}$ to the eight levels $4\,^{1,3}L$. For the three highest lying levels, namely $4\,^3\mathrm{F}$, $4\,^1\mathrm{F}$, $4\,^1\mathrm{P}$, our results lie above or very close to those of SB. For all the other transitions in Fig. 1 our results lie below SB's. This is not true at very low temperatures for $4-12$ and $4-14$. We find that $\Omega(4-12)$ has a narrow peak just above threshold energy and it is this pseudo resonance which causes $\Upsilon(4-12)$ to rise steeply as $T \to 0$. There are two transitions, namely $2\,^3\mathrm{P} \to 4\,^3\mathrm{D}$, $4\,^1\mathrm{D}$, for which the differences are of the order of a factor of 3. In Section 6 we give a physical explanation why SB's results and ours can sometimes differ by a large amount.

5. Stamp collection of collision strengths

We present some of our collision strengths graphically in the manner of a "stamp collection", each collision strength being plotted against the final electron energy within a small rectangle resembling a postage stamp. In this way we are able to put together 12 transitions per journal page. The present collision strengths contain structure in a narrow energy range which typically extends for 2 or 3 electron volts starting at threshold energy. Since we believe that these pseudo resonances (a) have no physical significance being an artefact of the CCC method and (b) only affect the thermally averaged collision strengths Υ at relatively low temperatures, we have not attempted to delineate them in great detail for most transitions.

An interesting result emerges from our calculations at low energies, namely that for some transitions the collision strengths appear to tend to finite non zero values

Table 2. Effective collision strengths for transitions in He: $1s^2\ ^1S \rightarrow 1s\ nl\ ^{1,3}L$ with $n = 2, 3, 4, 5$ and $l = 0, 1, 2, 3, 4$

$\log T$	Transition	$n=2$	$n=3$	$n=4$	$n=5$	Transition	$n=2$	$n=3$	$n=4$	$n=5$
3.75	$1^1S - n^1S$	3.075^{-2}	8.431^{-3}	2.397^{-3}	1.000^{-3}	$1^1S - n^3S$	6.198^{-2}	1.642^{-2}	5.317^{-3}	2.593^{-3}
4.00		3.492^{-2}	8.308^{-3}	2.505^{-3}	1.084^{-3}		6.458^{-2}	1.584^{-2}	5.233^{-3}	2.542^{-3}
4.25		3.840^{-2}	8.364^{-3}	2.642^{-3}	1.189^{-3}		6.387^{-2}	1.530^{-2}	5.183^{-3}	2.477^{-3}
4.50		4.183^{-2}	8.696^{-3}	2.856^{-3}	1.334^{-3}		6.157^{-2}	1.486^{-2}	5.179^{-3}	2.448^{-3}
4.75		4.573^{-2}	9.313^{-3}	3.178^{-3}	1.526^{-3}		5.832^{-2}	1.434^{-2}	5.142^{-3}	2.421^{-3}
5.00		5.048^{-2}	1.022^{-2}	3.628^{-3}	1.771^{-3}		5.320^{-2}	1.346^{-2}	4.936^{-3}	2.325^{-3}
5.25		5.649^{-2}	1.147^{-2}	4.210^{-3}	2.068^{-3}		4.787^{-2}	1.198^{-2}	4.461^{-3}	2.108^{-3}
5.50		6.436^{-2}	1.318^{-2}	4.941^{-3}	2.426^{-3}		4.018^{-2}	9.968^{-3}	3.738^{-3}	1.774^{-3}
5.75		7.481^{-2}	1.553^{-2}	5.888^{-3}	2.868^{-3}		3.167^{-2}	7.741^{-3}	2.904^{-3}	1.384^{-3}
3.75	$1^1S - n^1P$	8.886^{-3}	2.783^{-3}	1.046^{-3}	6.597^{-4}	$1^1S - n^3P$	1.716^{-2}	6.041^{-3}	2.074^{-3}	1.193^{-3}
4.00		1.299^{-2}	3.678^{-3}	1.504^{-3}	9.203^{-4}		2.233^{-2}	6.906^{-3}	2.468^{-3}	1.466^{-3}
4.25		1.910^{-2}	5.128^{-3}	2.143^{-3}	1.223^{-3}		2.826^{-2}	7.931^{-3}	2.983^{-3}	1.762^{-3}
4.50		3.006^{-2}	7.760^{-3}	3.173^{-3}	1.701^{-3}		3.477^{-2}	9.178^{-3}	3.585^{-3}	2.070^{-3}
4.75		5.178^{-2}	1.295^{-2}	5.180^{-3}	2.673^{-3}		4.128^{-2}	1.059^{-2}	4.236^{-3}	2.378^{-3}
5.00		9.534^{-2}	2.343^{-2}	9.287^{-3}	4.706^{-3}		4.635^{-2}	1.185^{-2}	4.796^{-3}	2.625^{-3}
5.25		1.778^{-1}	4.340^{-2}	1.713^{-3}	8.605^{-3}		4.800^{-2}	1.240^{-2}	5.048^{-3}	2.704^{-3}
5.50		3.167^{-1}	7.716^{-2}	3.040^{-2}	1.521^{-2}		4.503^{-2}	1.184^{-2}	4.832^{-3}	2.545^{-3}
5.75		5.217^{-1}	1.274^{-1}	5.023^{-2}	2.515^{-2}		3.808^{-2}	1.020^{-2}	4.169^{-3}	2.166^{-3}
3.75	$1^1S - n^1D$		3.884^{-3}	1.416^{-3}	7.906^{-4}	$1^1S - n^3D$		1.863^{-3}	1.030^{-3}	8.023^{-4}
4.00			3.809^{-3}	1.442^{-3}	8.285^{-4}			2.060^{-3}	1.125^{-3}	8.630^{-4}
4.25			3.783^{-3}	1.548^{-3}	8.888^{-4}			2.202^{-3}	1.247^{-3}	9.306^{-4}
4.50			3.942^{-3}	1.764^{-3}	1.009^{-3}			2.322^{-3}	1.354^{-3}	9.867^{-4}
4.75			4.390^{-3}	2.152^{-3}	1.230^{-3}			2.396^{-3}	1.407^{-3}	9.957^{-4}
5.00			5.266^{-3}	2.790^{-3}	1.585^{-3}			2.372^{-3}	1.389^{-3}	9.480^{-4}
5.25			6.598^{-3}	3.642^{-3}	2.047^{-3}			2.195^{-3}	1.283^{-3}	8.485^{-4}
5.50			8.159^{-3}	4.521^{-3}	2.522^{-3}			1.860^{-3}	1.087^{-3}	7.044^{-4}
5.75			9.556^{-3}	5.222^{-3}	2.900^{-3}			1.434^{-3}	8.368^{-4}	5.371^{-4}
3.75	$1^1S - n^1F$			5.864^{-4}	4.221^{-4}	$1^1S - n^3F$			5.082^{-4}	5.039^{-4}
4.00				4.917^{-4}	3.813^{-4}				4.547^{-4}	4.501^{-4}
4.25				4.101^{-4}	3.488^{-4}				3.748^{-4}	3.664^{-4}
4.50				3.467^{-4}	3.149^{-4}				2.945^{-4}	2.801^{-4}
4.75				3.011^{-4}	2.797^{-4}				2.268^{-4}	2.078^{-4}
5.00				2.697^{-4}	2.472^{-4}				1.724^{-4}	1.525^{-4}
5.25				2.436^{-4}	2.179^{-4}				1.279^{-4}	1.111^{-4}
5.50				2.135^{-4}	1.881^{-4}				9.081^{-5}	7.878^{-5}
5.75				1.781^{-4}	1.564^{-4}				6.114^{-5}	5.335^{-5}
3.75	$1^1S - n^1G$				1.938^{-4}	$1^1S - n^3G$				3.037^{-4}
4.00					1.551^{-4}					2.389^{-4}
4.25					1.158^{-4}					1.717^{-4}
4.50					8.143^{-5}					1.157^{-4}
4.75					5.484^{-5}					7.485^{-5}
5.00					3.640^{-5}					4.734^{-5}
5.25					2.473^{-5}					2.968^{-5}
5.50					1.742^{-5}					1.860^{-5}
5.75					1.244^{-5}					1.197^{-5}

Table 3. Effective collision strengths for transitions in He: $1s\,2s\ ^3S \rightarrow 1s\ nl\ ^{1,3}L$ with $n = 2, 3, 4, 5$ and $l = 0, 1, 2, 3, 4$

$\log T$	Transition	$n=2$	$n=3$	$n=4$	$n=5$	Transition	$n=2$	$n=3$	$n=4$	$n=5$
3.75	$2^3S - n^1S$	2.389	3.544^{-1}	1.199^{-1}	5.624^{-2}	$2^3S - n^3S$		2.410	6.651^{-1}	2.321^{-1}
4.00		2.456	3.295^{-1}	1.062^{-1}	4.930^{-2}			2.286	5.911^{-1}	2.154^{-1}
4.25		2.275	2.832^{-1}	8.877^{-2}	4.129^{-2}			2.235	5.383^{-1}	2.001^{-1}
4.50		1.916	2.280^{-1}	7.059^{-2}	3.305^{-2}			2.370	5.328^{-1}	2.009^{-1}
4.75		1.496	1.730^{-1}	5.351^{-2}	2.517^{-2}			2.761	5.919^{-1}	2.265^{-1}
5.00		1.111	1.247^{-1}	3.870^{-2}	1.823^{-2}			3.397	7.092^{-1}	2.732^{-1}
5.25		8.003^{-1}	8.624^{-2}	2.682^{-2}	1.261^{-2}			4.187	8.591^{-1}	3.302^{-1}
5.50		5.660^{-1}	5.765^{-2}	1.793^{-2}	8.402^{-3}			5.013	1.016	3.889^{-1}
5.75		3.944^{-1}	3.747^{-2}	1.165^{-2}	5.419^{-3}			5.755	1.163	4.443^{-1}
3.75	$2^3S - n^1P$	7.965^{-1}	1.306^{-1}	4.941^{-2}	3.272^{-2}	$2^3S - n^3P$	1.508^{+1}	1.606	4.476^{-1}	1.833^{-1}
4.00		9.579^{-1}	1.499^{-1}	5.791^{-2}	3.599^{-2}		2.580^{+1}	1.611	4.465^{-1}	1.936^{-1}
4.25		1.042	1.543^{-1}	6.089^{-2}	3.587^{-2}		4.185^{+1}	1.576	4.476^{-1}	2.015^{-1}
4.50		1.015	1.439^{-1}	5.740^{-2}	3.259^{-2}		6.455^{+1}	1.552	4.578^{-1}	2.105^{-1}
4.75		8.950^{-1}	1.234^{-1}	4.930^{-2}	2.730^{-2}		9.526^{+1}	1.615	4.938^{-1}	2.291^{-1}
5.00		7.265^{-1}	9.896^{-2}	3.939^{-2}	2.141^{-2}		1.351^{+2}	1.868	5.842^{-1}	2.707^{-1}
5.25		5.516^{-1}	7.494^{-2}	2.964^{-2}	1.586^{-2}		1.842^{+2}	2.410	7.603^{-1}	3.493^{-1}
5.50		3.948^{-1}	5.367^{-2}	2.106^{-2}	1.114^{-2}		2.401^{+2}	3.274	1.037	4.719^{-1}
5.75		2.677^{-1}	3.639^{-2}	1.419^{-2}	7.434^{-3}		2.976^{+2}	4.382	1.408	6.315^{-1}
3.75	$2^3S - n^1D$		2.479^{-1}	8.385^{-2}	4.285^{-2}	$2^3S - n^3D$		1.392	3.528^{-1}	1.678^{-1}
4.00			2.591^{-1}	8.375^{-2}	4.240^{-2}			1.954	4.605^{-1}	2.013^{-1}
4.25			2.558^{-1}	8.145^{-2}	4.053^{-2}			2.760	6.158^{-1}	2.496^{-1}
4.50			2.375^{-1}	7.635^{-2}	3.781^{-2}			3.900	8.407^{-1}	3.309^{-1}
4.75			2.071^{-1}	6.833^{-2}	3.398^{-2}			5.496	1.182	4.661^{-1}
5.00			1.694^{-1}	5.755^{-2}	2.874^{-2}			7.599	1.672	6.649^{-1}
5.25			1.292^{-1}	4.502^{-2}	2.253^{-2}			9.990	2.262	9.058^{-1}
5.50			9.188^{-2}	3.264^{-2}	1.635^{-2}			1.226^{+1}	2.841	1.143
5.75			6.137^{-2}	2.212^{-2}	1.108^{-2}			1.408^{+1}	3.319	1.339
3.75	$2^3S - n^1F$			4.106^{-2}	2.766^{-2}	$2^3S - n^3F$			3.325^{-1}	1.840^{-1}
4.00				4.019^{-2}	2.809^{-2}				3.889^{-1}	2.165^{-1}
4.25				3.838^{-2}	2.713^{-2}				4.620^{-1}	2.564^{-1}
4.50				3.475^{-2}	2.450^{-2}				5.534^{-1}	3.066^{-1}
4.75				2.954^{-2}	2.068^{-2}				6.671^{-1}	3.692^{-1}
5.00				2.341^{-2}	1.628^{-2}				7.814^{-1}	4.329^{-1}
5.25				1.719^{-2}	1.192^{-2}				8.556^{-1}	4.769^{-1}
5.50				1.175^{-2}	8.147^{-3}				8.707^{-1}	4.903^{-1}
5.75				7.577^{-3}	5.257^{-3}				8.385^{-1}	4.774^{-1}
3.75	$2^3S - n^1G$				1.409^{-2}	$2^3S - n^3G$				8.969^{-2}
4.00					1.175^{-2}					8.533^{-2}
4.25					9.224^{-3}					7.928^{-2}
4.50					6.900^{-3}					7.392^{-2}
4.75					4.932^{-3}					6.903^{-2}
5.00					3.359^{-3}					6.279^{-2}
5.25					2.181^{-3}					5.440^{-2}
5.50					1.360^{-3}					4.498^{-2}
5.75					8.284^{-4}					3.616^{-2}

Table 4. Effective collision strengths for transitions in He: $1s\,2s\ ^1S \rightarrow 1s\ nl\ ^{1,3}L$ with $n = 2, 3, 4, 5$ and $l = 0, 1, 2, 3, 4$

$\log T$	Transition	$n=2$	$n=3$	$n=4$	$n=5$	Transition	$n=2$	$n=3$	$n=4$	$n=5$
3.75	$2^1S - n^1S$		5.290^{-1}	1.237^{-1}	4.939^{-2}	$2^1S - n^3S$		6.360^{-1}	2.118^{-1}	8.235^{-2}
4.00			5.736^{-1}	1.268^{-1}	4.801^{-2}			5.308^{-1}	1.753^{-1}	7.071^{-2}
4.25			6.711^{-1}	1.371^{-1}	5.053^{-2}			4.177^{-1}	1.368^{-1}	5.659^{-2}
4.50			8.581^{-1}	1.667^{-1}	6.149^{-2}			3.131^{-1}	1.017^{-1}	4.293^{-2}
4.75			1.149	2.224^{-1}	8.346^{-2}			2.252^{-1}	7.260^{-2}	3.113^{-2}
5.00			1.526	2.990^{-1}	1.137^{-1}			1.566^{-2}	4.992^{-2}	2.164^{-2}
5.25			1.940	3.836^{-1}	1.467^{-1}			1.061^{-2}	3.325^{-2}	1.449^{-2}
5.50			2.344	4.653^{-1}	1.782^{-1}			7.073^{-2}	2.161^{-2}	9.418^{-3}
5.75			2.705	5.373^{-1}	2.063^{-1}			4.654^{-2}	1.378^{-2}	5.987^{-3}
3.75	$2^1S - n^1P$	1.099^{+1}	2.806^{-1}	8.756^{-2}	4.363^{-2}	$2^1S - n^3P$	1.591	4.914^{-1}	1.520^{-1}	5.736^{-2}
4.00		1.929^{+1}	3.409^{-1}	1.136^{-1}	5.476^{-2}		1.728	4.684^{-1}	1.437^{-1}	5.789^{-2}
4.25		3.097^{+1}	4.246^{-1}	1.480^{-1}	6.919^{-2}		1.735	4.092^{-1}	1.273^{-1}	5.383^{-2}
4.50		4.628^{+1}	5.629^{-1}	1.945^{-1}	8.892^{-2}		1.579	3.304^{-1}	1.053^{-1}	4.629^{-2}
4.75		6.536^{+1}	8.352^{-1}	2.694^{-1}	1.208^{-1}		1.310	2.503^{-1}	8.195^{-2}	3.715^{-2}
5.00		8.828^{+1}	1.374	4.034^{-1}	1.769^{-1}		1.008	1.806^{-1}	6.048^{-2}	2.803^{-2}
5.25		1.146^{+2}	2.301	6.265^{-1}	2.685^{-1}		7.297^{-1}	1.250^{-1}	4.251^{-2}	1.996^{-2}
5.50		1.430^{+2}	3.638	9.482^{-1}	3.996^{-1}		5.015^{-1}	8.311^{-2}	2.850^{-2}	1.347^{-2}
5.75		1.719^{+2}	5.299	1.354	5.658^{-1}		3.292^{-1}	5.312^{-2}	1.829^{-2}	8.677^{-3}
3.75	$2^1S - n^1D$		8.375^{-1}	2.070^{-1}	7.112^{-2}	$2^1S - n^3D$		2.596^{-1}	7.885^{-2}	4.162^{-2}
4.00			1.167	2.355^{-1}	8.076^{-2}			3.050^{-1}	8.766^{-2}	4.405^{-2}
4.25			1.675	2.874^{-1}	9.700^{-2}			3.263^{-1}	9.224^{-2}	4.461^{-2}
4.50			2.438	3.808^{-1}	1.296^{-1}			3.166^{-1}	9.066^{-2}	4.341^{-2}
4.75			3.529	5.415^{-1}	1.893^{-1}			2.824^{-1}	8.324^{-2}	4.007^{-2}
5.00			4.941	7.779^{-1}	2.781^{-1}			2.332^{-1}	7.090^{-2}	3.430^{-2}
5.25			6.494	1.058	3.829^{-1}			1.782^{-1}	5.558^{-2}	2.693^{-2}
5.50			7.930	1.328	4.830^{-1}			1.265^{-1}	4.019^{-2}	1.947^{-2}
5.75			9.070	1.548	5.637^{-1}			8.433^{-2}	2.714^{-2}	1.312^{-2}
3.75	$2^1S - n^1F$			1.837^{-1}	8.834^{-2}	$2^1S - n^3F$			5.952^{-2}	3.836^{-2}
4.00				2.230^{-1}	1.039^{-1}				6.338^{-2}	4.042^{-2}
4.25				2.829^{-1}	1.295^{-1}				6.369^{-2}	4.009^{-2}
4.50				3.657^{-1}	1.681^{-1}				5.925^{-2}	3.707^{-2}
4.75				4.717^{-1}	2.204^{-1}				5.112^{-2}	3.201^{-2}
5.00				5.799^{-1}	2.762^{-1}				4.083^{-2}	2.568^{-2}
5.25				6.564^{-1}	3.192^{-1}				3.011^{-2}	1.903^{-2}
5.50				6.864^{-1}	3.409^{-1}				2.062^{-2}	1.310^{-2}
5.75				6.807^{-1}	3.443^{-1}				1.330^{-2}	8.484^{-3}
3.75	$2^1S - n^1G$				4.146^{-2}	$2^1S - n^3G$				2.367^{-2}
4.00					4.233^{-2}					1.929^{-2}
4.25					4.377^{-2}					1.507^{-2}
4.50					4.673^{-2}					1.140^{-2}
4.75					4.971^{-2}					8.329^{-3}
5.00					5.011^{-2}					5.804^{-3}
5.25					4.685^{-2}					3.842^{-3}
5.50					4.115^{-2}					2.429^{-3}
5.75					3.499^{-2}					1.486^{-3}

Table 5. Effective collision strengths for transitions in He: $1s\,2p\ ^3P \rightarrow 1s\ nl\ ^{1,3}L$ with $n = 2, 3, 4, 5$ and $l = 0, 1, 2, 3, 4$

$\log T$	Transition	$n=2$	$n=3$	$n=4$	$n=5$	Transition	$n=2$	$n=3$	$n=4$	$n=5$
3.75	$2^3P - n^1S$		6.756^{-1}	2.971^{-1}	1.446^{-1}	$2^3P - n^3S$		5.858	2.192	5.585^{-1}
4.00			6.387^{-1}	2.664^{-1}	1.276^{-1}			5.614	1.778	5.196^{-1}
4.25			5.623^{-1}	2.255^{-1}	1.074^{-1}			5.828	1.513	4.854^{-1}
4.50			4.633^{-1}	1.801^{-1}	8.586^{-2}			7.035	1.432	4.860^{-1}
4.75			3.582^{-1}	1.359^{-1}	6.503^{-2}			9.926	1.587	5.507^{-1}
5.00			2.610^{-1}	9.742^{-2}	4.678^{-2}			1.524^{+1}	2.026	6.982^{-1}
5.25			1.803^{-1}	6.655^{-2}	3.204^{-2}			2.332^{+1}	2.750	9.268^{-1}
5.50			1.188^{-1}	4.351^{-2}	2.097^{-2}			3.372^{+1}	3.700	1.217
5.75			7.516^{-2}	2.738^{-2}	1.320^{-2}			4.549^{+1}	4.797	1.549
3.75	$2^3P - n^1P$	3.689	8.012^{-1}	2.403^{-1}	1.246^{-1}	$2^3P - n^3P$		1.295^{+1}	3.340	1.101
4.00		4.259	8.612^{-1}	2.671^{-1}	1.370^{-1}			1.325^{+1}	3.265	1.151
4.25		4.507	8.397^{-1}	2.699^{-1}	1.374^{-1}			1.399^{+1}	3.278	1.215
4.50		4.321	7.465^{-1}	2.475^{-1}	1.253^{-1}			1.555^{+1}	3.471	1.329
4.75		3.800	6.137^{-1}	2.082^{-1}	1.051^{-1}			1.815^{+1}	3.912	1.527
5.00		3.135	4.752^{-1}	1.637^{-1}	8.244^{-2}			2.177^{+1}	4.586	1.804
5.25		2.464	3.510^{-1}	1.218^{-1}	6.106^{-2}			2.600^{+1}	5.404	2.125
5.50		1.857	2.479^{-1}	8.619^{-2}	4.297^{-2}			3.031^{+1}	6.240	2.444
5.75		1.346	1.674^{-1}	5.809^{-2}	2.886^{-2}			3.425^{+1}	6.988	2.727
3.75	$2^3P - n^1D$		1.333	4.536^{-1}	2.103^{-1}	$2^3P - n^3D$		1.003^{+1}	2.860	1.357
4.00			1.353	4.278^{-1}	1.998^{-1}			1.438^{+1}	3.613	1.587
4.25			1.303	3.940^{-1}	1.832^{-1}			2.173^{+1}	4.820	1.961
4.50			1.192	3.539^{-1}	1.639^{-1}			3.489^{+1}	6.907	2.676
4.75			1.032	3.074^{-1}	1.426^{-1}			5.878^{+1}	1.071^{+1}	4.041
5.00			8.388^{-1}	2.534^{-1}	1.180^{-1}			9.961^{+1}	1.725^{+1}	6.387
5.25			6.339^{-1}	1.949^{-1}	9.106^{-2}			1.610^{+2}	2.697^{+1}	9.836
5.50			4.467^{-1}	1.394^{-1}	6.532^{-2}			2.404^{+2}	3.937^{+1}	1.418^{+1}
5.75			2.965^{-1}	9.361^{-2}	4.392^{-2}			3.309^{+2}	5.344^{+1}	1.908^{+1}
3.75	$2^3P - n^1F$			2.011^{-1}	1.565^{-1}	$2^3P - n^3F$			2.400	1.364
4.00				1.921^{-1}	1.445^{-1}				2.836	1.533
4.25				1.830^{-1}	1.306^{-1}				3.497	1.809
4.50				1.683^{-1}	1.147^{-1}				4.478	2.253
4.75				1.458^{-1}	9.666^{-2}				5.866	2.906
5.00				1.170^{-1}	7.659^{-2}				7.490	3.693
5.25				8.647^{-2}	5.636^{-2}				8.936	4.422
5.50				5.919^{-2}	3.863^{-2}				9.920	4.966
5.75				3.814^{-2}	2.499^{-2}				1.043^{+1}	5.240
3.75	$2^3P - n^1G$				6.174^{-2}	$2^3P - n^3G$				6.103^{-1}
4.00					5.161^{-2}					5.874^{-1}
4.25					4.157^{-2}					5.743^{-1}
4.50					3.257^{-2}					5.844^{-1}
4.75					2.459^{-2}					6.035^{-1}
5.00					1.758^{-2}					6.009^{-1}
5.25					1.181^{-2}					5.601^{-1}
5.50					7.523^{-3}					4.928^{-1}
5.75					4.597^{-3}					4.207^{-1}

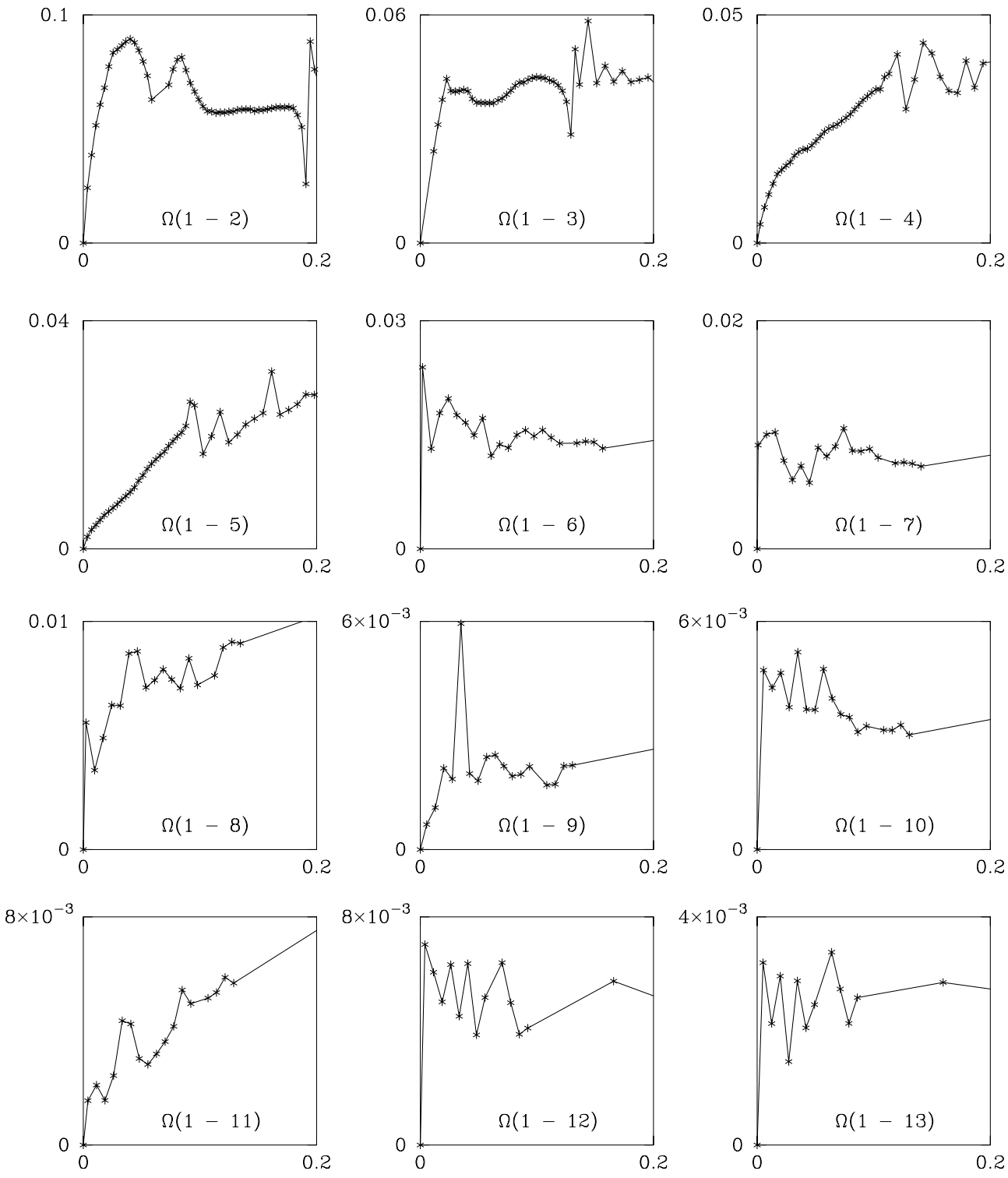

Fig. 2. CCC collision strengths vs. final energy in Ry

at threshold. However this behaviour may simply arise because of pseudo resonances since there is no apparent physical explanation for it. When carrying out the thermal averaging we impose the condition that all our collision strengths be zero at threshold.

Figures 2, 4, 6, 8, 10 show collision strengths for transitions $1 \rightarrow 2$, ... $2 \rightarrow 29$ with the final electron energy varying from zero to 0.2 rydbergs (2.72 eV). Figures 3, 5, 7, 9, 11 are for the same 55 transitions but with the final collision energy now going from 0.2 Ry to 1 Ry

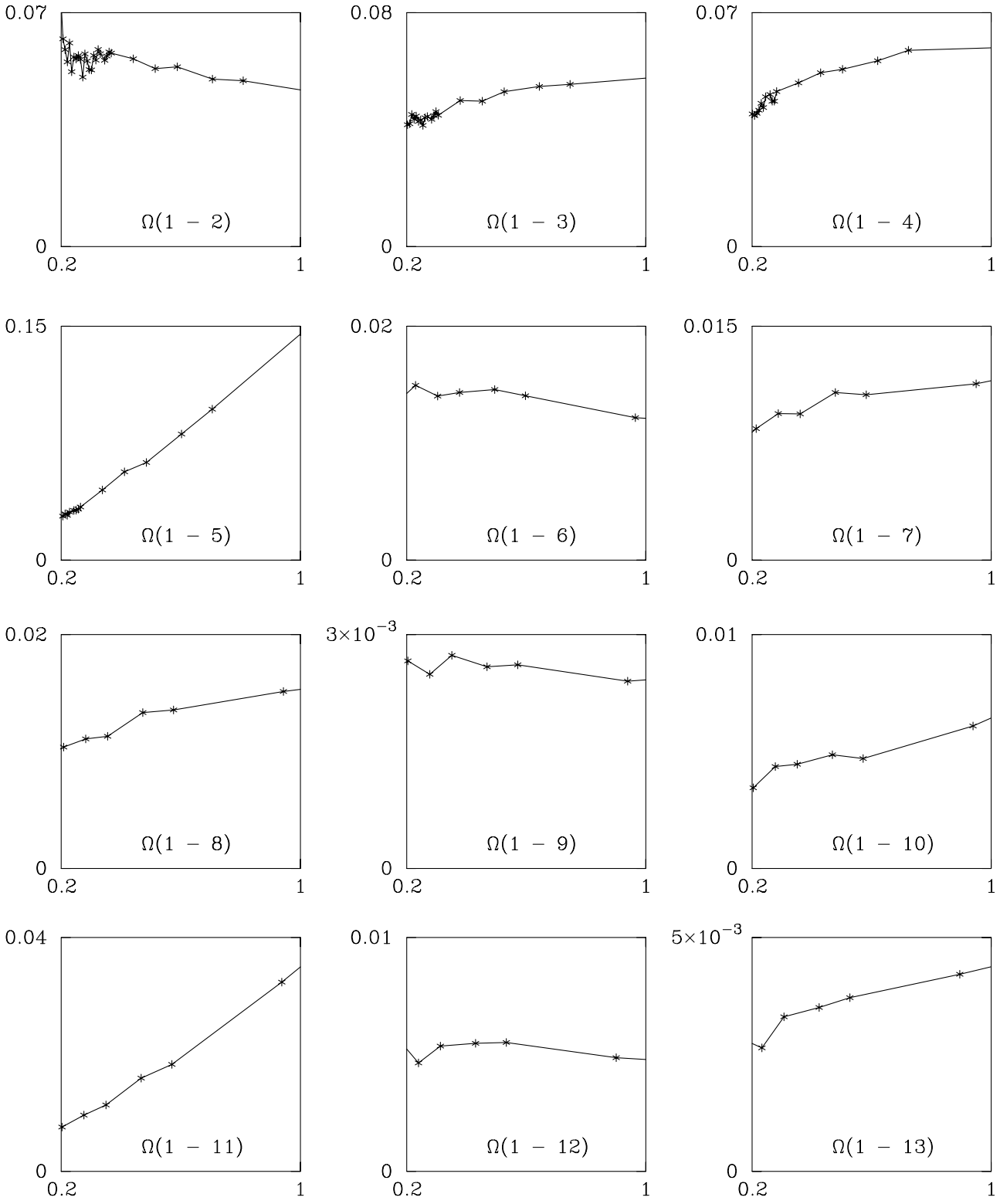

Fig. 3. CCC collision strengths vs. final energy in Ry

(13.6058 eV). It should be noted that the vertical scale varies from one "stamp" to another and is chosen in order to optimise the legibility. Pseudo resonances can be seen in most of the low energy "stamps", i.e. when the final electron energy is between 0 and 0.2 Ry. The occasional irregularities occurring above 0.2 Ry are presumably also produced by pseudo resonances.

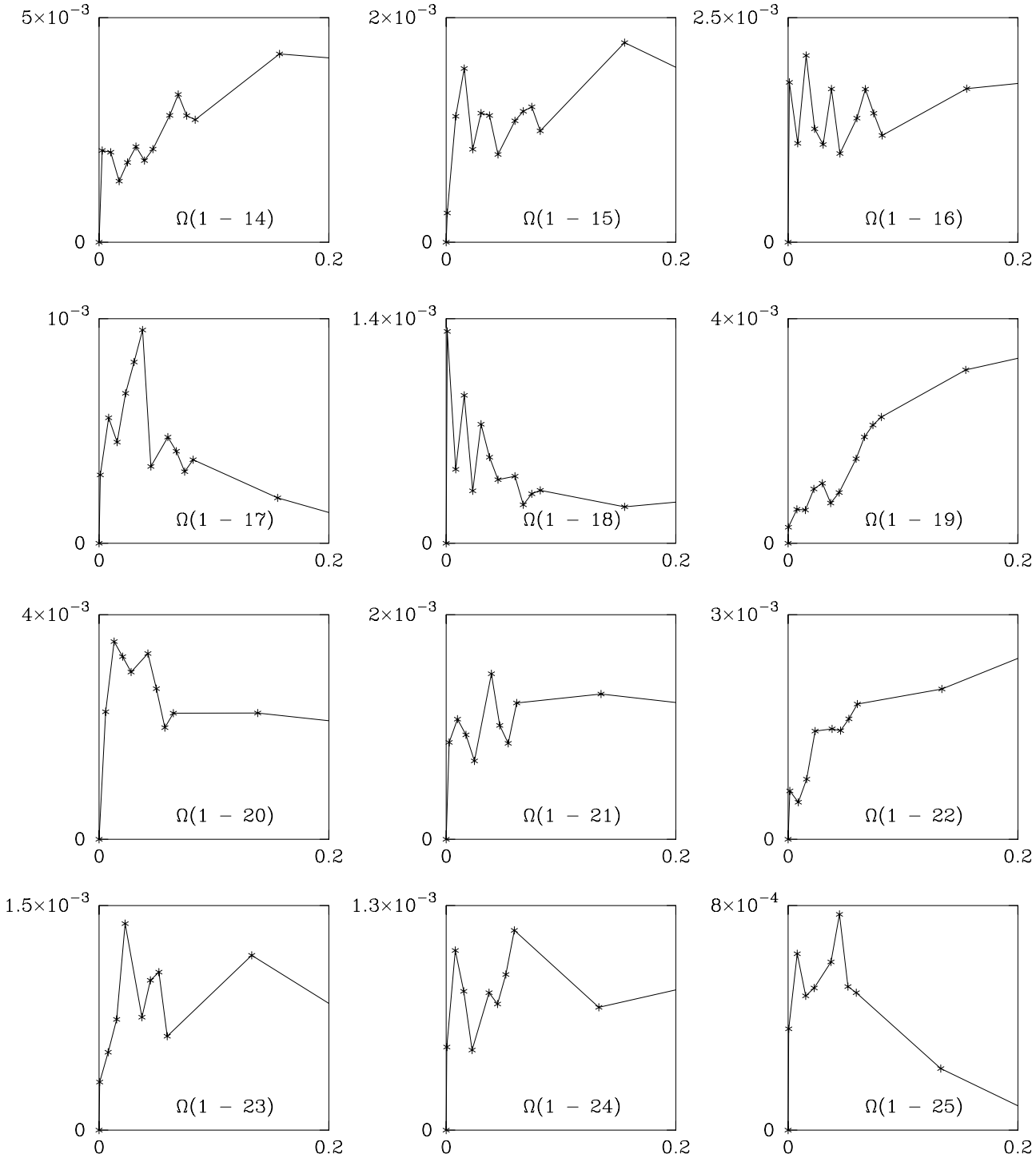

Fig. 4. CCC collision strengths vs. final energy in Ry

Collision strengths for electron excitation of neutral atoms do not contain the enormous amount of resonance structure associated with positive ions: see, for example, Hummer et al. (1993). There is some structure, but we have considered it to be of secondary importance in so far as the thermally averaged collision strengths $\Upsilon(i-j)$

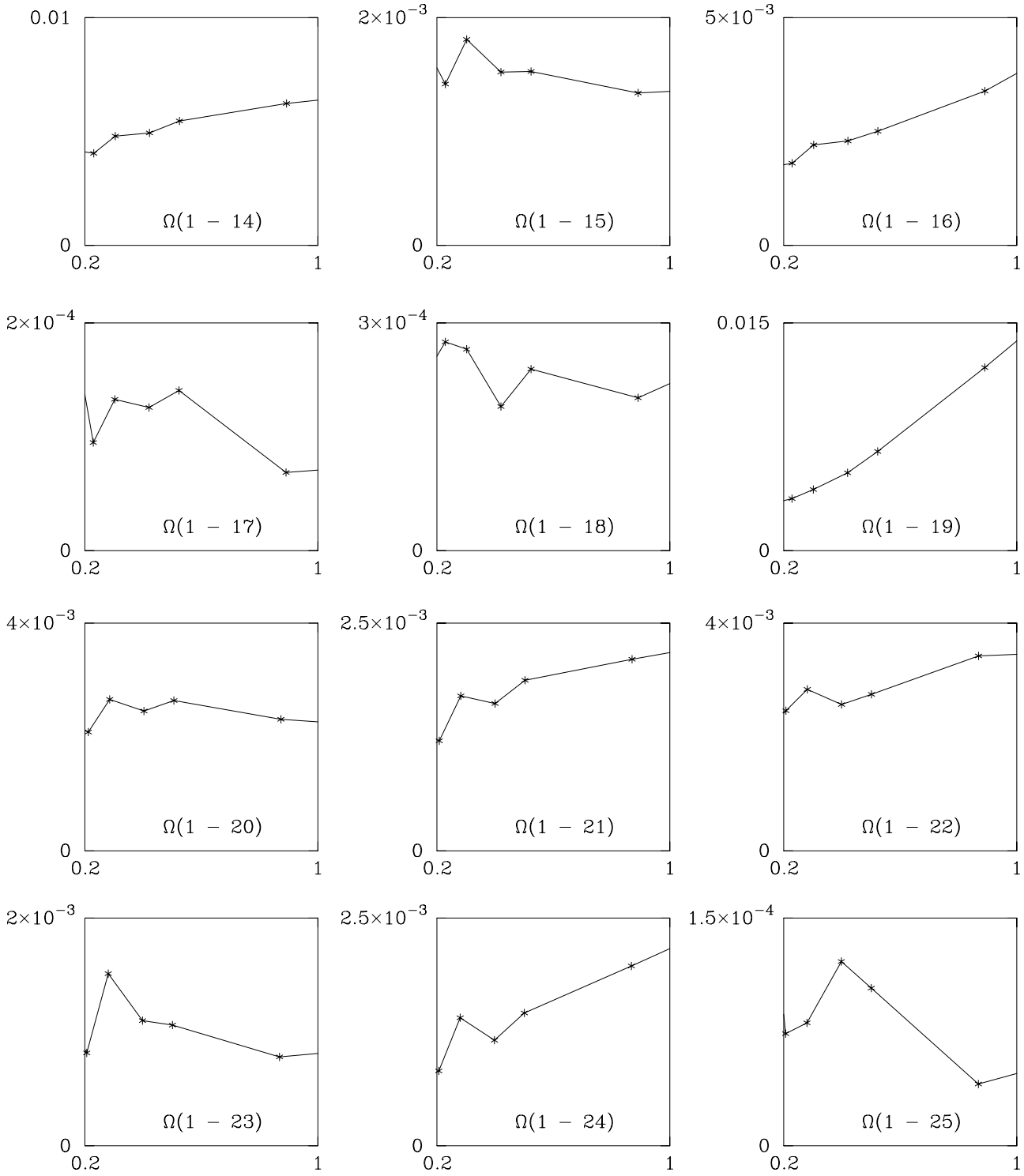

Fig. 5. CCC collision strengths vs. final energy in Ry

are concerned. It would be too costly in computer time to attempt to delineate the structure associated with each transition. Also this structure tends to occur over a limited energy range just above threshold energy.

6. Assessing the reliability

Although in Tables 2 − 5 we give results with 4 significant figures we need to warn the reader against believing that this reflects the reliability of our data.

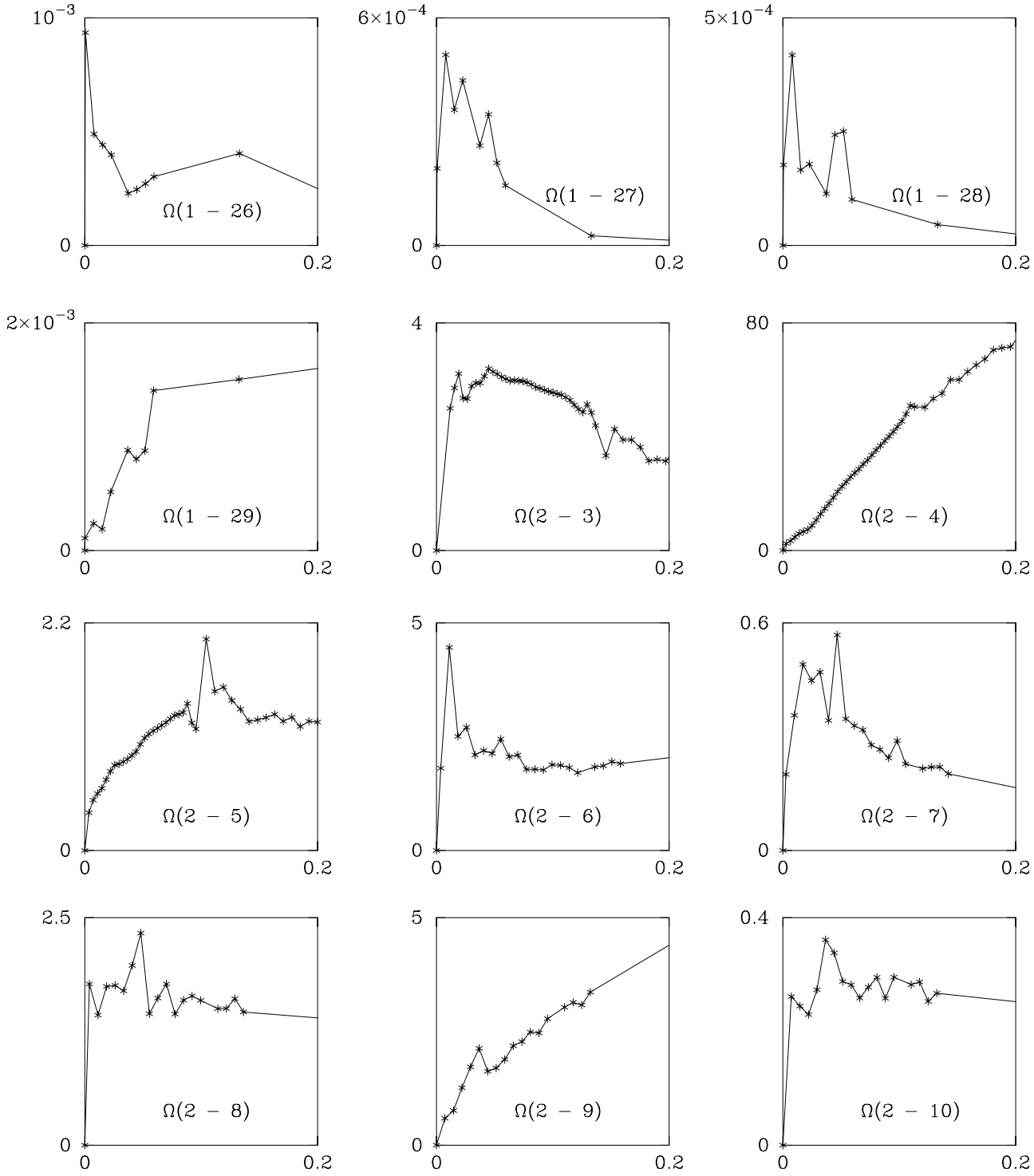

Fig. 6. CCC collision strengths vs. final energy in Ry

At low temperatures the value obtained for $\Upsilon(T)$ depends quite critically on the energy dependence of the cross section near threshold. Since the target is a neutral atom, $\Omega(E_j) \propto E_j^{1/2}$ for sufficiently small E_j, but, for most of the transitions, the data produced by the CCC calculations are not sufficiently detailed at low energies

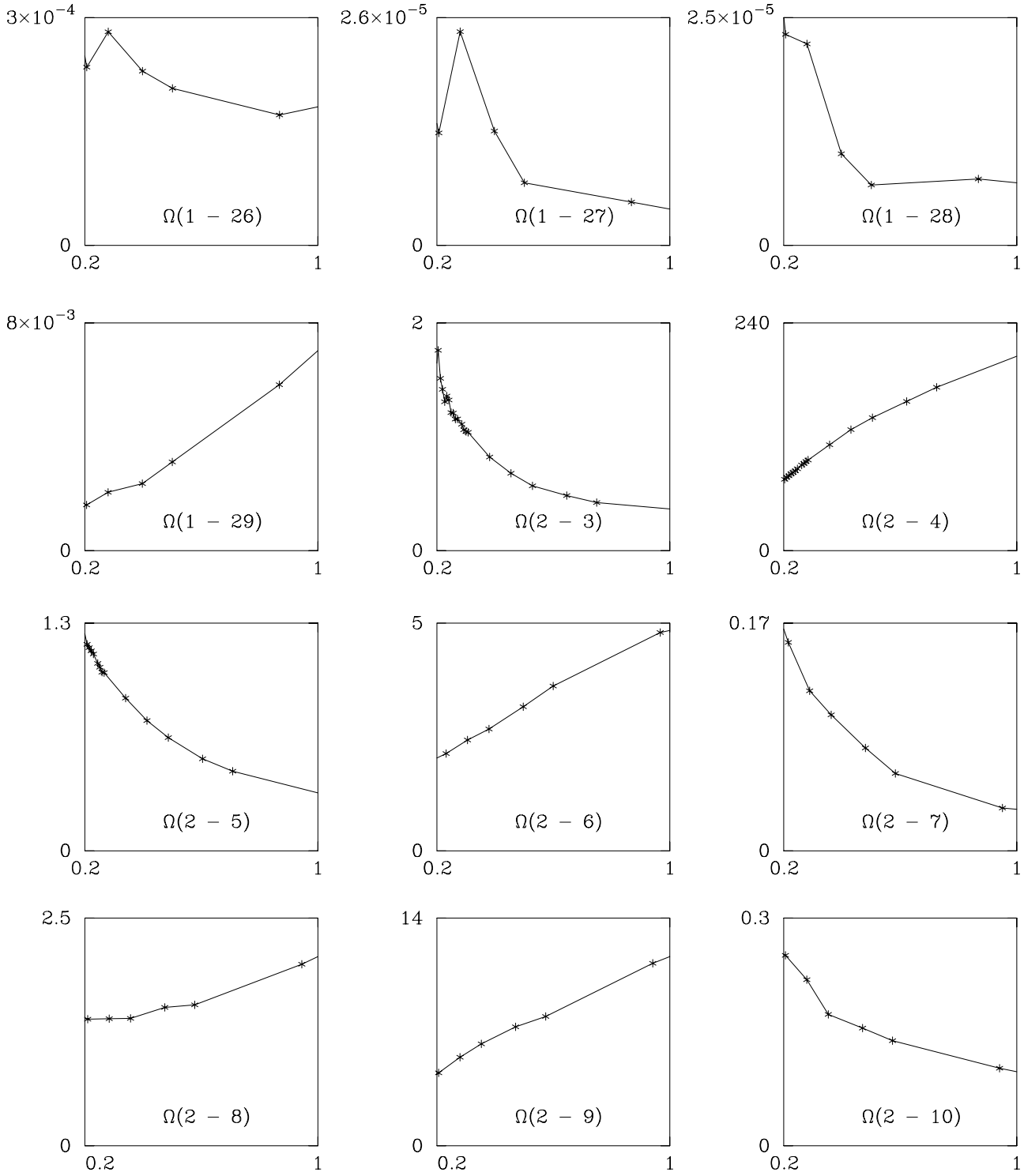

Fig. 7. CCC collision strengths vs. final energy in Ry

to delineate this. The numbers given here for $\Upsilon(T)$ were obtained by assuming that $\Omega(E_j)$ falls linearly to zero in the interval between $E_j = 0$ and the lowest value of E_j at which the cross section was calculated. For our tabulated range, we have $\log T \geq 3.75$, where the error due to this threshold effect does not exceed a few percent. Further details will be given elsewhere.

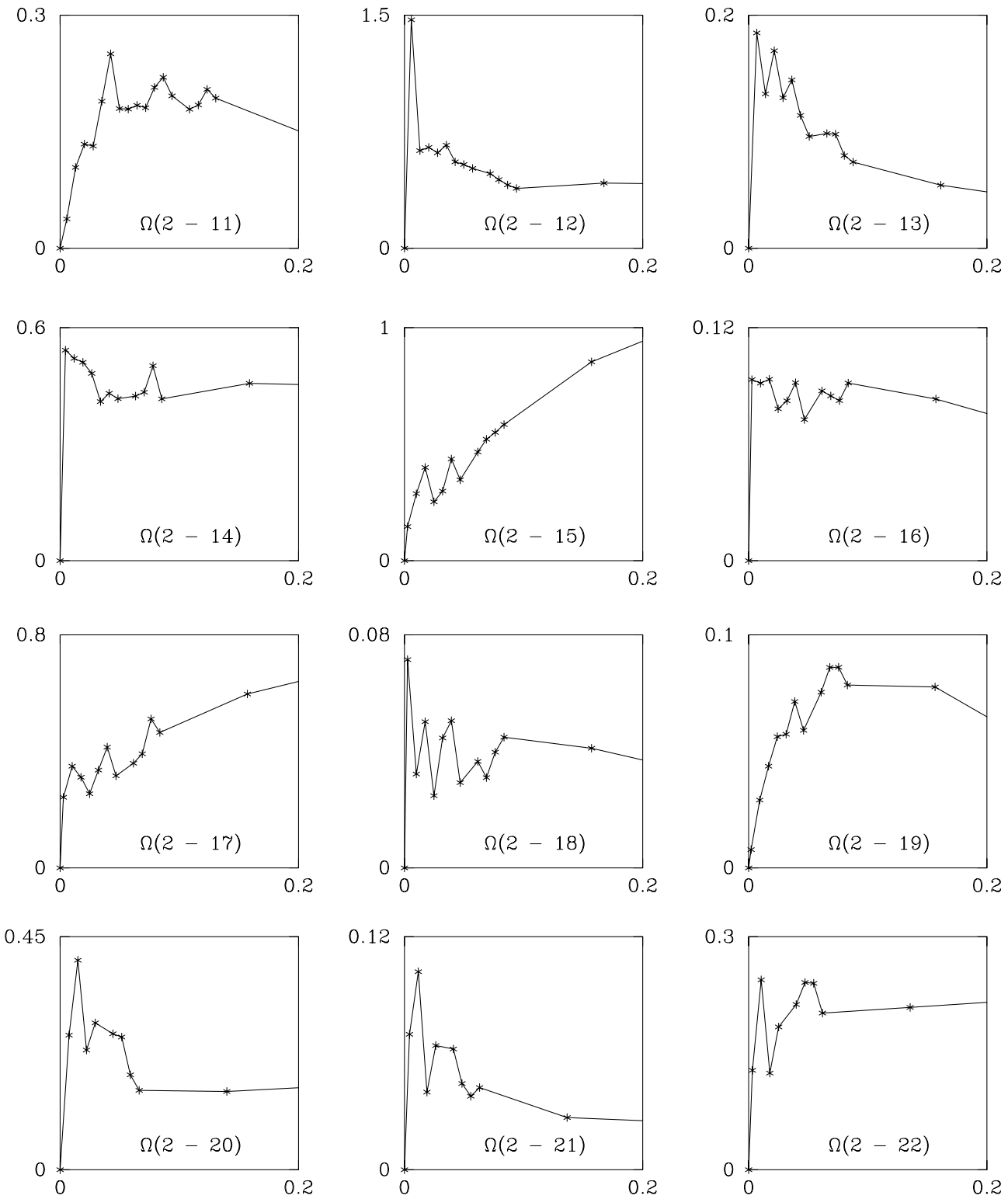

Fig. 8. CCC collision strengths vs. final energy in Ry

The CCC approximation takes full account of continuum states, whereas the R-matrix method used by both BK and SB does not. Allowing for the continua has two opposite effects: (a) part of the flux which would go to discrete states is now diverted towards continuum states, so reducing collision strengths for transitions between discrete states; (b) intermediate continuum states may provide alternative routes for flux to reach discrete states,

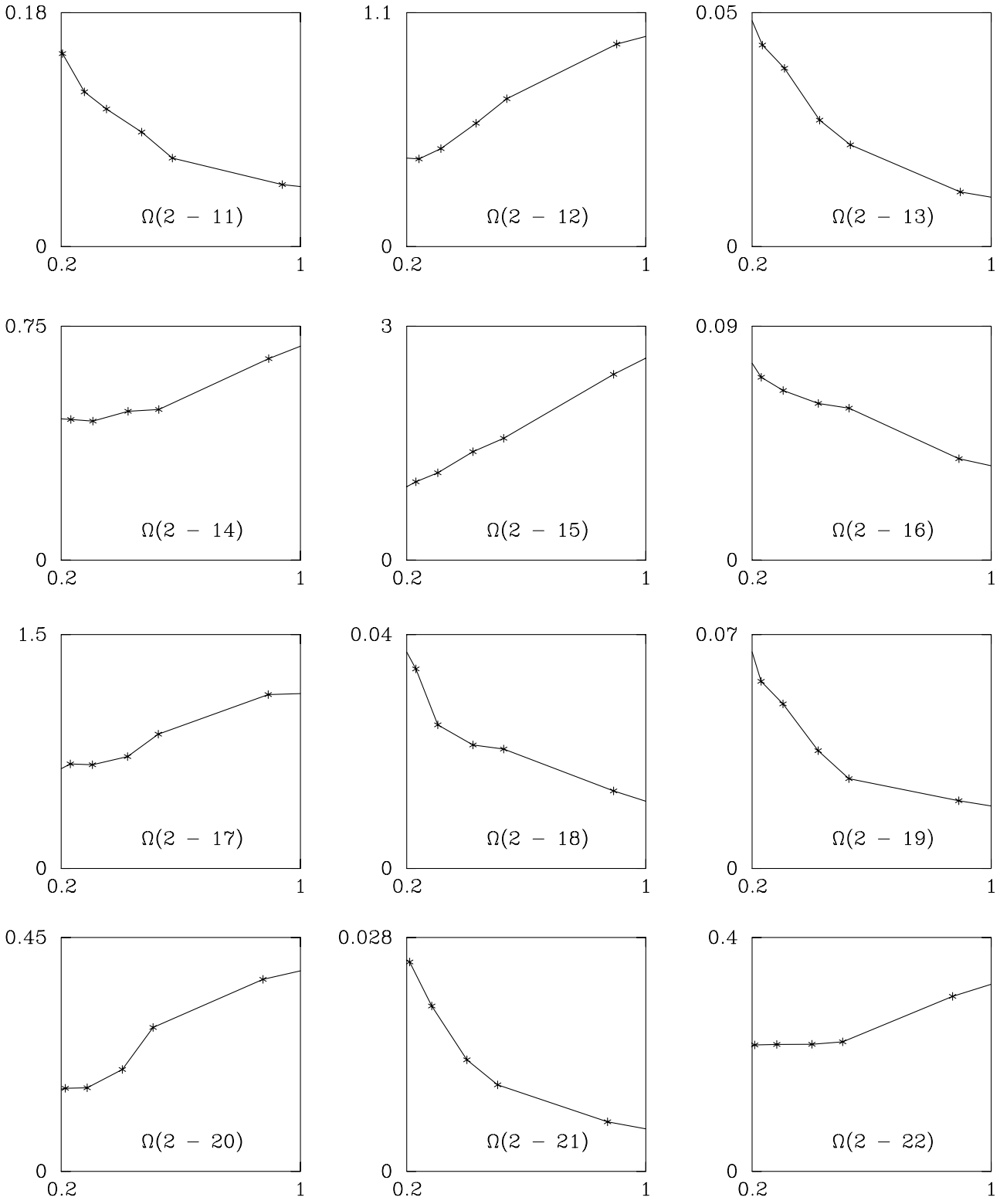

Fig. 9. CCC collision strengths vs. final energy in Ry

thereby increasing collision strengths. By comparing effective collision strengths we reach the following conclusions: for transitions $1 \rightarrow j$, $2 \rightarrow j$, $3 \rightarrow j$ the ratio Υ(BBFT)/Υ(SB) is close to one for $j \leq 11$, and is significantly less than one if $j \geq 12$ (i.e. $n = 4$). This we interpret to mean that (a) is the dominant effect for these latter transitions. However, for some of the $4 \rightarrow j$ transitions the ratio is appreciably greater than one,

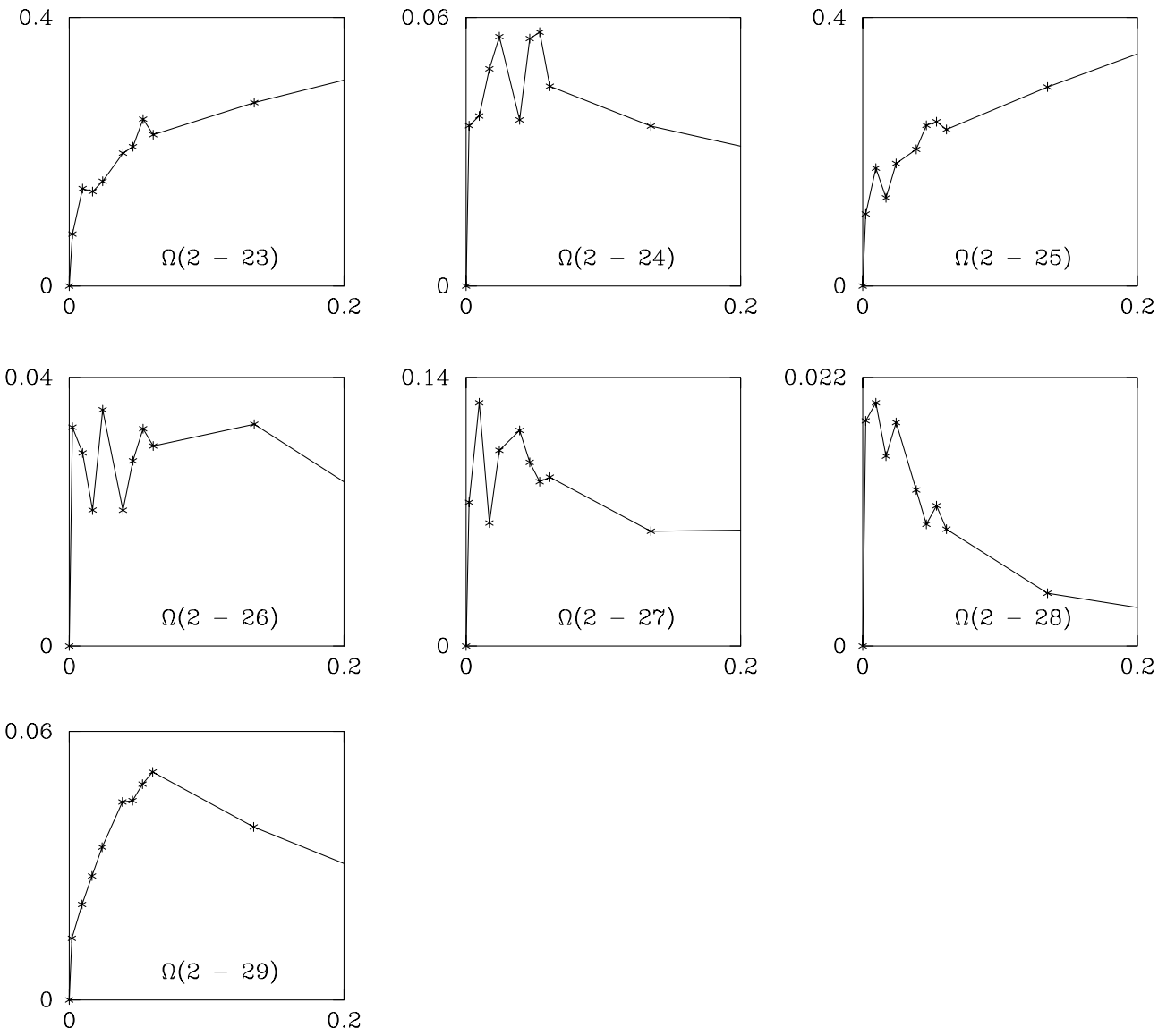

Fig. 10. CCC collision strengths vs. final energy in Ry

indicating that (b) dominates. This suggests that the continuum states are capable of either decreasing or increasing collision strengths particularly if both the initial and final levels are close to the ionisation threshold.

7. On the history of the discovery of helium

In view of the misrepresentation given in many books on astronomy, (see for example Payne-Gaposhkin & Haramundanis 1970; Celnikier 1986; Zirin 1988; Phillips 1992), we feel it is worthwhile saying a few words here on the subject of who discovered helium. The British astronomer Joseph Norman Lockyer gives the first documented account (Lockyer 1869a,b,c) of a hitherto unknown bright chromospheric yellow line which was later known to have been produced by helium. Lockyer observed the chromosphere in October 1868 and not during the solar eclipse of 18 August 1868; he labelled the yellow line D^3 but was unable to identify the element giving rise to it. Lockyer used a technique devised independently by himself and by the French astronomer Pierre Jules César Janssen to observe the chromospheric spectrum outside of an eclipse. Janssen made observations in India during the August eclipse of 1868 but did not record the yellow line that Lockyer saw 2 months later. So credit for the discovery of helium in the Sun should go to Lockyer, not to Janssen. Aubin (1999) has given a detailed account of this fascinating episode in the history of astronomy.

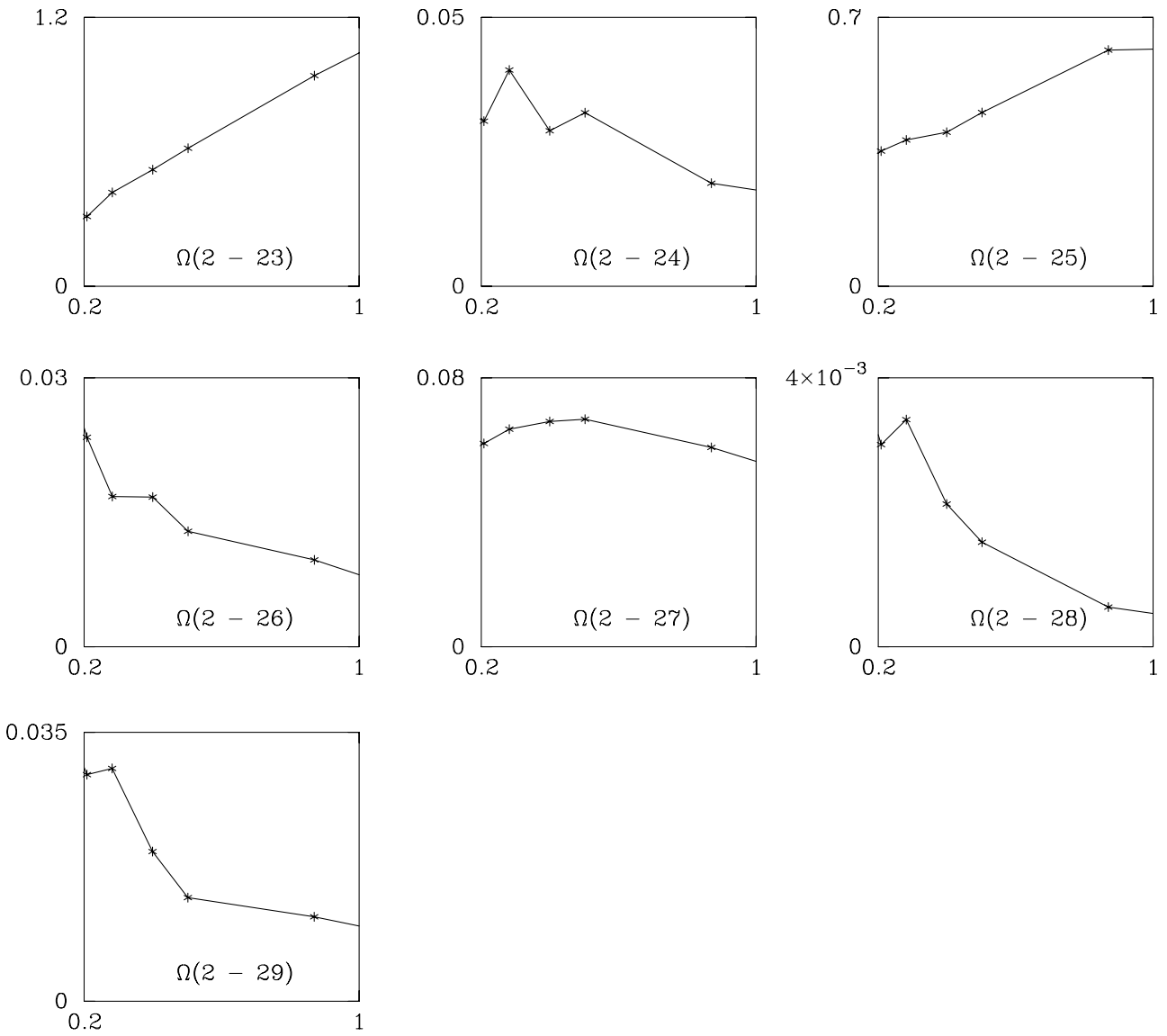

Fig. 11. CCC collision strengths vs. final energy in Ry

Acknowledgements. David G. Hummer of Boulder (Colorado) gave the initial encouragement for undertaking the present investigation. Klaus Bartschat of Des Moines (Indiana) kindly provided us with his cross sections and details of the model helium atom he used. Jean-Claude Bouret of Toulouse (France) pointed out to us the astronomical importance of electron-helium rate coefficients at temperatures in excess of 30 000 degrees, while Hugh P. Summers of Glasgow (Scotland) drew our attention to the needs of those working in the field of Controlled Thermonuclear Energy. We drew all of the figures using the software package TVB developed by Georges Gonczi at the Observatoire de la Côte d'Azur; this is freely available at http://www.obs-nice.fr/tvb/tvb.html with instructions now given in English. Robert P. McEachran of Toronto (Canada) provided the frozen-core Hartree-Fock energies in Table 1. Thanks to the painstaking care with which our anonymous referee examined the original draft, we were alerted of some slip-ups in Table 3 and so able to correct them prior to publication.

References

Aubin D., 1999, La Recherche 321, 78
Bartschat K., 1998, J. Phys. B 31, L469
Bartschat K., Hudson E.T., Scott M.P., et al., 1996, J. Phys. B 29, 115
Bartschat K., 1999 (private communication)
Berrington K.A., Kingston A.E., 1987, J. Phys. B 20, 6621
Bouret J.-C., 1998 (private communication)
Burgess A., Tully J.A., 1992, A&A 254, 436
Celnikier L.M., 1986, "Histoire de l'Astronomie occidentale", Technique et Documentation. Lavoisier, Paris
Cohen M., McEachran R.P., 1967a, Proc. Phys. Soc. 92, 37

Cohen M., McEachran R.P., 1967b, Proc. Phys. Soc. 92, 539
Fursa D.V., Bray I., 1995, Phys. Rev. A 52, 1279
Hummer D.G., Berrington K.A., Eissner W., et al., 1993, A&AS 279, 298
Lockyer J.N., 1869a, MNRAS 29, 90
Lockyer J.N., 1869b, Phil. Trans. Roy. Soc. Lond. 159, 425
Lockyer J.N., 1869c, Proc. Roy. Soc. Lond. 17, 131
McEachran R.P., 1972 (private communication)
McEachran R.P., Cohen M., 1969, J. Phys. B 2, 1271
Martin W.C., 1973, J. Phys. Chem. Ref. Data 2, 257
Payne-Gaposchkin C., Haramundanis K., 1970, "Introduction to Astronomy". Prentice-Hall International, Inc., New Jersey
Phillips K.J.H., 1992, "Guide to the sun". Cambridge University Press
Pradhan A.K., 1987, Proceedings of Atomic Data Workshop: Assessment of data for photo-ionization and photo-excitation and for electron impact excitation of atomic ions. Eissner W., Kingston A.E. (eds.). Science & Engineering Research Council, Daresbury Laboratory, Daresbury, Warrington WA4 4AD, UK
Sawey P.M.J., Berrington K.A., 1993, Atom. Data Nucl. Data Tables 55, 81
Sawey P.M.J., Berrington K.A., Burke P.G., Kingston A.E., 1990, J. Phys. B 23, 4321
Seaton M.J., 1953, Proc. Roy. Soc. A 218, 400
Summers H.P., 1999 (private communication)
Zirin H., 1988, "Astrophysics of the Sun". Cambridge University Press